Electronic Supplementary Information (ESI)

Evidenced cucurbit[n]uril-based host–guest interactions using single-molecule force spectroscopy

Mingyang Zhang, *Hao Zhang, Lunqiang Jin, Hao Li, Simin Liu, Shuai Chang,* and Feng Liang**

The State Key Laboratory of Refractories and Metallurgy, School of Chemistry and Chemical Engineering, Wuhan University of Science and Technology, Wuhan 430081, P. R. China

E-mail: schang23@wust.edu.cn (S.C.);

feng_liang@whu.edu.cn (F.L.)

M. Zhang and H. Zhang contributed equally to this work.

Experimental Section:

1. Chemicals Syntheses

General Information

All the reagents and solvents were purchased from commercial sources and used as received unless otherwise noted. Compounds **G1-3**, **AZO**, and **MV2** were synthesized according to our reported procedures[S1-S3]. The **G4** (FGGC) was purchased from Shanghai Mujin Biological Technology Co., Ltd. Ultrapure water was produced by Experimental Water System (Lab-UV-20) and used in our measurements. ^{1}H NMR spectra were recorded on a Bruker AVANCE III 600 MHz NMR spectrometer at 25 °C. Ultraviolet-visible (UV-Vis) spectra were recorded on a Shimadzu UV-2550 instrument. SMFS was taken with keysight SPM6500. The power of UV light (365 nm) and visible light (450 nm) are both 5 W.

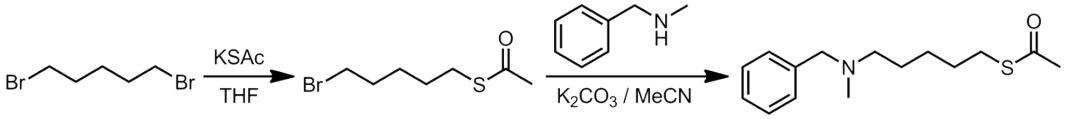

Scheme S1. Synthetic route to **G1**.

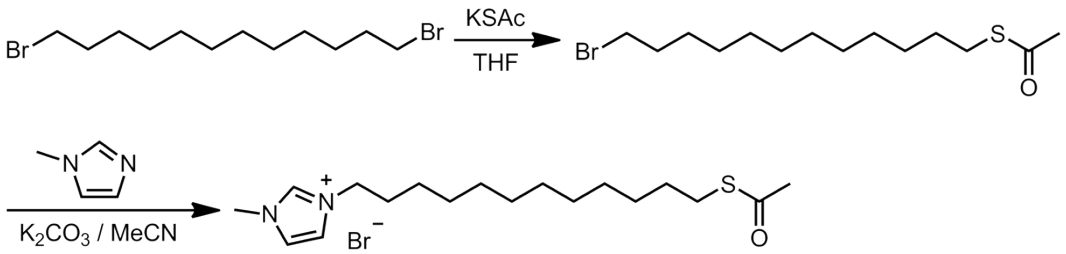

Scheme S2. Synthetic route to **G2**.

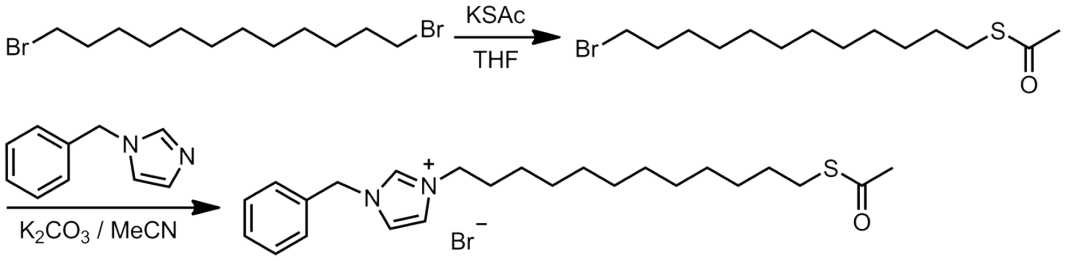

Scheme S3. Synthetic route to **G3**.

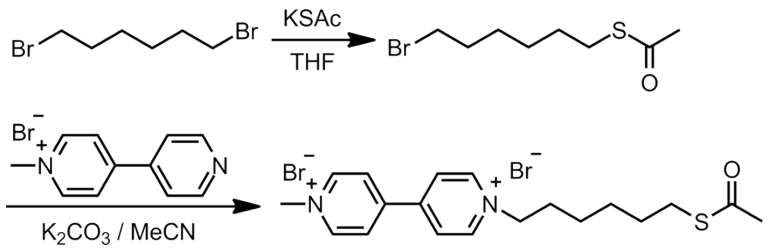

Scheme S4. Synthetic route to **MV1**.

Synthesis of G1:[S3] 1,5-Dibromopentane (18.0 g; 78.6 mmol) was added to a solution of potassium thiolacetate (1.52 g; 80.0 mmol) in THF (80 mL), and the reaction mixture was refluxed for 20 h under N_2. Then, the mixture was cooled down to room temperature, resulting in precipitation of a solid. The solid was collected by filtration, washed with THF, and purified on a silicagel column (hexane/dichloromethane = 2/1) as a colorless oil (S-(5-bromopentyl) ethanethioate). ^{1}H NMR ($CDCl_3$, 600 MHz, δ): 3.38 (t, *J*=7.1 Hz, 2H), 2.85 (t, *J*=7.1 Hz, 2H), 2.30 (s, 3H), 1.91-1.81 (m, *J*=7.1 Hz, 2H), 1.67-1.54 (m, 2H).

To S-(5-bromopentyl)ethanethioate (1.2 g, 5.0 mmol) and K_2CO_3 (2.0 g, 15 mmol) in 40 mL of MeCN was added N-benzylmethylamine (0.72 g, 6 mmol). The resulting solution was heated at reflux for 10 h. The solvent was removed under reduced pressure. And the residue was purified on a silicagel column (Petroleum ether/ethyl acetate = 5/1) as a colorless oil. ^{1}H NMR ($CDCl_3$, 600 MHz, δ): 7.34-7.18 (m, *J*=7.5 Hz, 5H), 3.45 (s, 2H), 2.86 (t, *J*=7.1 Hz, 2H), 2.35-2.32 (t, J=7.1 Hz, 2H), 2.29 (s, 3H), 2.15 (s, 3H), 1.57 (m, *J*=7.1 Hz 2H), 1.50 (m, *J*=7.1 Hz 2H), 1.40-1.32 (m, 2H).

Synthesis of G2:[S3] **G2** was synthesized following the same method for synthesizing **G1**. Product was obtained by using 1,12-Dibromododecane and 1-Methylimidazole instead of 1,5-dibromopentane and N-benzylmethylamine. ^{1}H NMR (D_2O, 600 MHz, δ): 8.74 (s, 1H), 7.50 (m, 1H), 7.46 (m, 1H), 4.21 (m, *J*=7.1 Hz, 2H), 3.91 (s, 3H), 2.90 (m, *J*=7.1 Hz, 2H), 2.38 (s, 3H), 1.89 (m, *J*=7.1 Hz, 2H), 1.59 (m, *J*=7.1 Hz, 2H), 1.39-1.29 (m, 16H).

Synthesis of G3:[S3] **G3** was synthesized following the same method for synthesizing **G2**. Product was obtained by using 1-benzyl-1H-imidazole instead of 1-Methylimidazole. ^{1}H NMR (D_2O, 600 MHz, δ):9.04 (s, 1H), 7.58 (m, 1H), 7.55 (m, 1H), 7.44-7.32 (m, *J*=7.5 Hz, 5H), 5.44 (s, 2H), 4.24 (m, *J*=7.1 Hz, 2H), 2.80 (m, *J*=7.1 Hz, 2H) 2.28 (s, 3H), 1.80 (m, *J*=7.1 Hz, 2H), 1.51 (m, *J*=7.1 Hz, 2H), 1.30-1.15 (m, 16H).

Synthesis of MV1:[S13] **MV1** was synthesized following the same method for synthesizing **G1**. Product was obtained by using 1,6-dibromohexane and 1-methyl-[4,4'-bipyridin]-1-ium iodide instead of 1,5-dibromopentane and N-benzylmethylamine. ^{1}H NMR (D_2O, 600 MHz, δ): 9.14-9.07 (dd, *J*=7.5 Hz, 4H), 8.57-8.54 (dd, *J*=7.5 Hz, 4H), 4.53 (s, 3H), 3.24 (m, *J*=7.1 Hz, 2H), 2.38 (s, 3H), 2.11 (m, *J*=7.1 Hz, 2H). 1.69 (m, *J*=7.1 Hz, 2H), 1.49-1.37 (m, 6H).

2. SMFS Experimental detail

Cleaning of AFM tips

Before modification, the AFM tips were treated with piranha solution (H_2SO_4 (98%)/H_2O_2 (30%) =7:3 in volume) for 1 h, followed by thorough rinsing with ultrapure water for 5 min, and then rinsing with ethanol for 5 min, and dried by argon flow.

Modification of AFM tips

The tips were modified by 3-aminopropyltriethoxysilane (APTES) using vapor phase deposition method for 2h (usually 298 K). A heterobifunctional PEG linker (Maleimide-PEG-NHS) was attached by incubating the tip for 3 h in 0.15 mL of chloroform containing 1 mg Maleimide-PEG-NHS and 1% triethylamine, resulting in acylation of surface-linked maleimide by the N-hydroxysuccinimide (NHS) group. After rinsing with chloroform and drying, the tips were incubated in a mixture of 0.2 mL pyrolidine and 1 mL of 1 mM/L guest molecule solution (all guest molecules were hydrolysed by mild acid to remove thioesters and converted into the sulfhydryl groups before use). Then, 5 μL of 1 mM ethanolamine hydrochloride was added and

incubation was continued for 10 min to block unreacted aldehyde groups. Eventually, the modified tips are stored in ultra-pure water for up to seven days.

Preparation of Bare Au

The substrate was a 100 nm Au evaporated on mica by thermal evaporation system (Angstrom Engineering, Covap). Immediately before each experiment, we annealed the substrate by hydrogen flame to further remove possible contamination (**Figure S1a**). And also this procedure is known to result in atomically flat Au(111) terraces[S4].

Preparation of guest molecule modified substrates

G1, **G2**, **G3**, **G4** molecules were hydrolysed by mild acid to remove thioesters and converted into the sulfhydryl groups before use, then immerse the gold substrate in 1mM guest molecule solution for 12 hours. As can be seen from the STM image (**Figure S1b**), there are still many flat areas on the gold surface. Because CB[8] can be directly connected with gold, in order to prevent the interference of CB[8] added later in the experiment, we used mix solution to modify the substrate. The mixed guest-butanethiolate solution was prepared by mixing guest molecule and butanethiolate at 1:1 stoichiometry in DI water, followed by a treatment of sonication for ~5 minutes, then immerse the gold substrate in the mixed solution for 12 hours (**Figure S1c**). After that, the substrate was taken out, rinsed with DI water, dried with nitrogen gas, and used immediately.

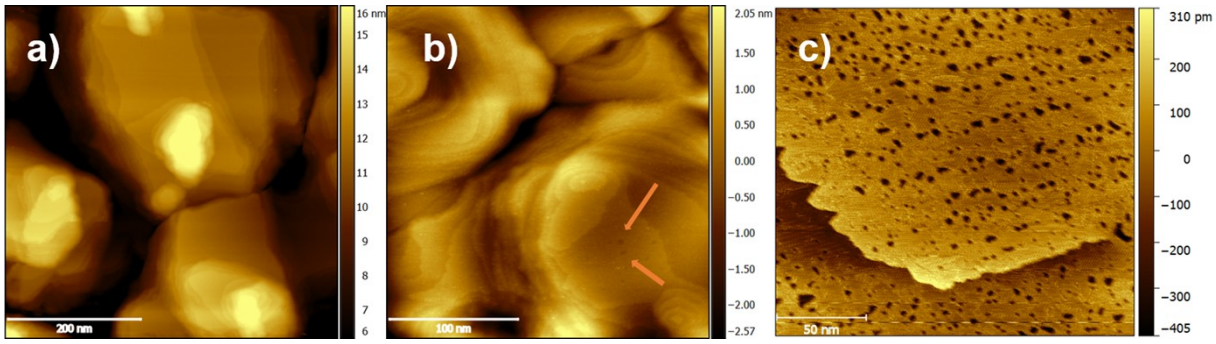

Figure S1. (a) STM image of bare Au. (b) STM image of Au substrate treated with **G1**. (c) STM image of Au substrate treated with **G1** and butanethiol, a random distribution of potholes

which depth is consistent with Au atom is packed the entire surface. Other molecules (**G2**, **G3**, **G4**, **MV1**) are modified on gold substrate with the same procedures.

AFM-based SMFS measurement and data analysis

Force spectroscopy experiments on both isolated single molecules and individual molecules in SAMs on gold were carried out on a Keysight SPM 6500 in contact mode. Functionalized Si_3N_4 AFM tips were adopted in this work, and the spring constants of AFM cantilevers were calibrated by the thermal noise method, producing spring constants of 0.02-0.03 N/m. As the rupture force was easily affected by temperature[S5], all measurements were carried out with freshly prepared AFM tips and samples in ultrapure water at room temperature (25 ℃). In each approach-retraction cycle, a modified AFM tip was first brought into contact with the gold surface with a same trip. During the separation of the AFM tip from substrate, the formed connective bridge can be stretched and eventually broken, and the rupture force can be recorded. The data is analyzed by Labview software, and the selected rupture force signal usually needs to follow these two rules: a) The rupture distance is less than 10nm, b) The pulling of PEG polymer should be observed before breaking, to exclude the interference of non-specific forces. Here, we used a PEG polymer chain to connect guest molecule to tip surface, which length is about 4nm, plus the length of APTES and guest molecule, so we don't pick rupture distance larger than 10 nm. Before the host-guest interaction break, there may be some non-specific force interference, so to determine whether the jump signal is true, in addition to the appropriate break length, also need to observe the typical polymer stretch curve[S6-S7].

AFM-based SMFS loading rate dependence

Here, different loading rates are used to test the interaction forces of the three host-guest systems, and their binding constants are calculated from SMFS data. And it has been confirmed that the measurement system is under kinetic control, because the rupture force increased with the increased loading rate[S8-S9]. When the tip speed is 0.5 μm/s, more signals are collected and the time of data collection is also appropriate, so the speed of 0.5 μm/s is used in the following

experiment[S6]. The loading rate is the tip speed times the tip spring constant, which is about 10^4 pN/s.

3. Experimental Data

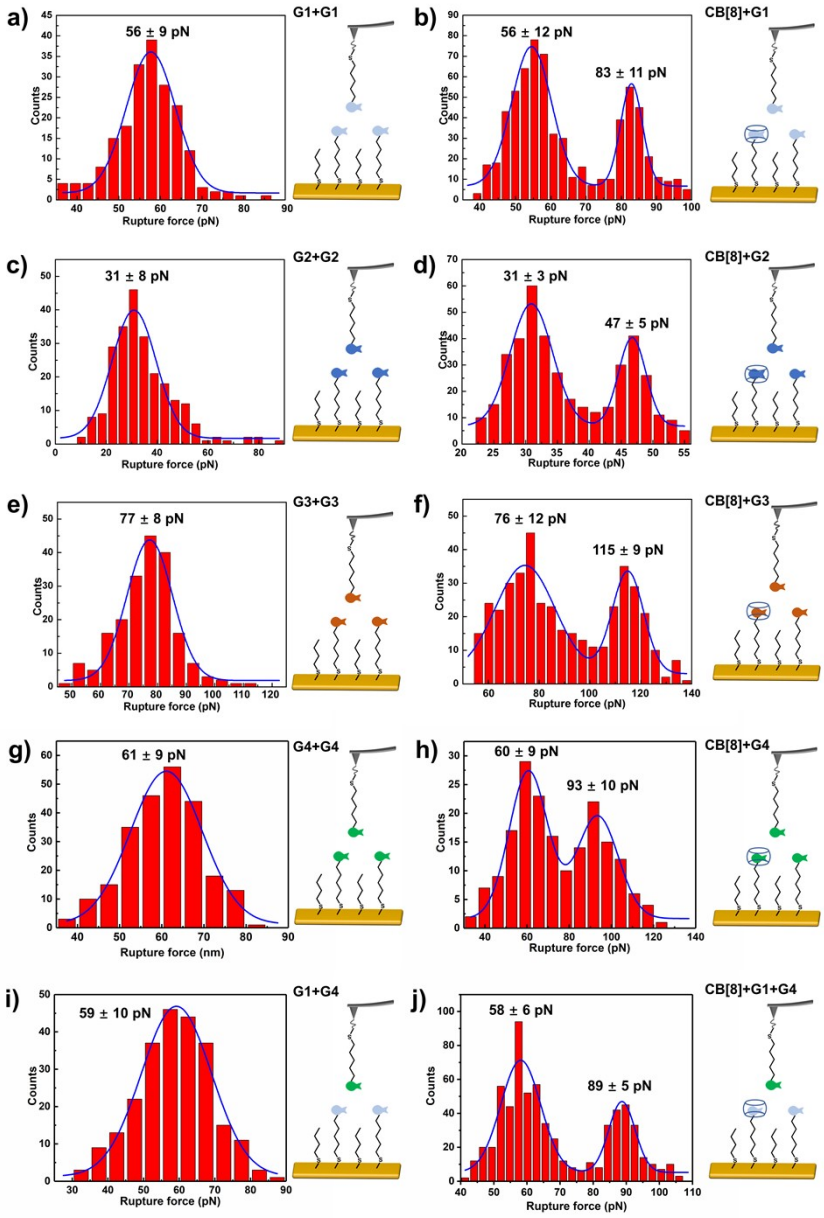

Figure S2. Histograms of the rupture force measured for the interaction between guest pairs without CB[8]: **(a) G1**, **(c) G2**, **(e) G3**, **(g) G4**, **(i) G1+G4**, and enhanced guest pairs interactions between guest pairs with CB[8]: **(b) G1**, **(d) G2**, **(f) G3**, **(h) G4**, and **(j) G1+G4**.

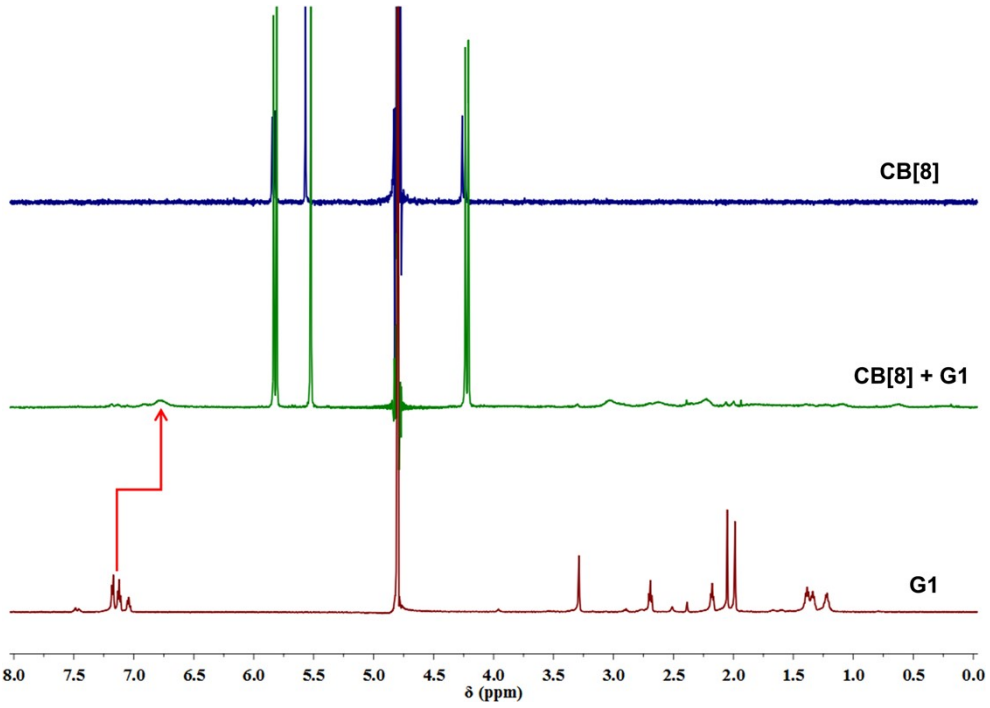

Figure S3. ^{1}H NMR spectra (D_2O, 600 MHz, 298K) of CB[8] (saturated solution), CB[8] (1 mM) and **G1** (2 mM), **G1** (2 mM).

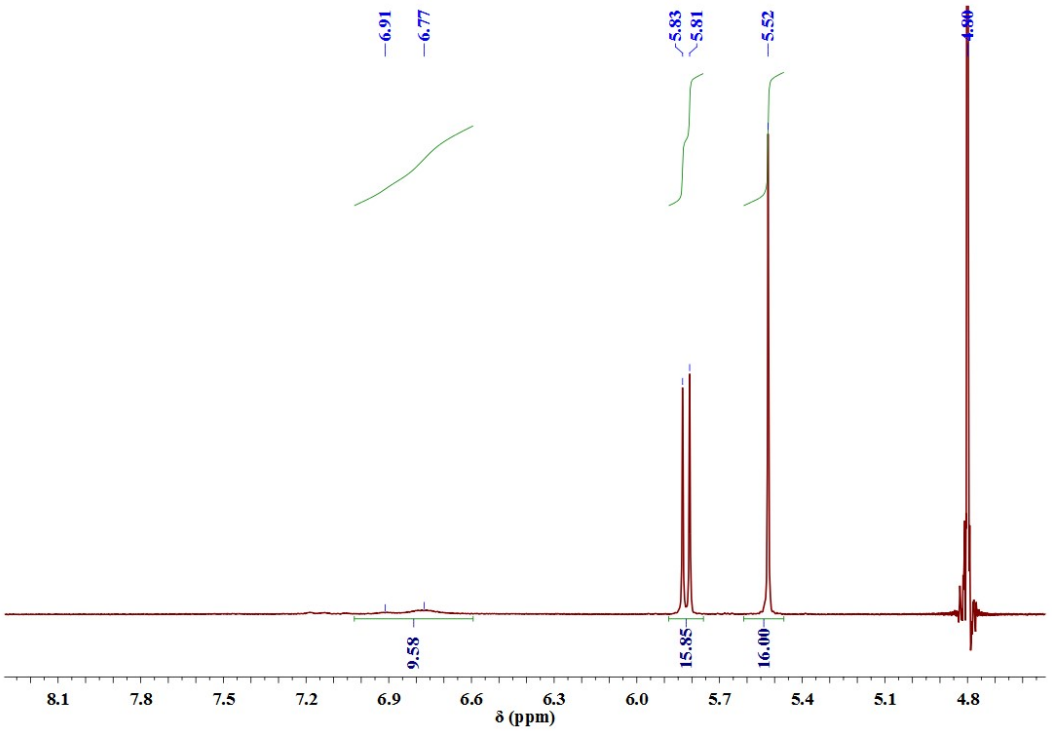

Figure S4. ^{1}H NMR spectrum (D_2O, 600 MHz, 298K) of CB[8] (1 mM) and **G1** (2 mM), confirming the 1:2 stoichiometry of CB[8] and **G1** by the integral of H.

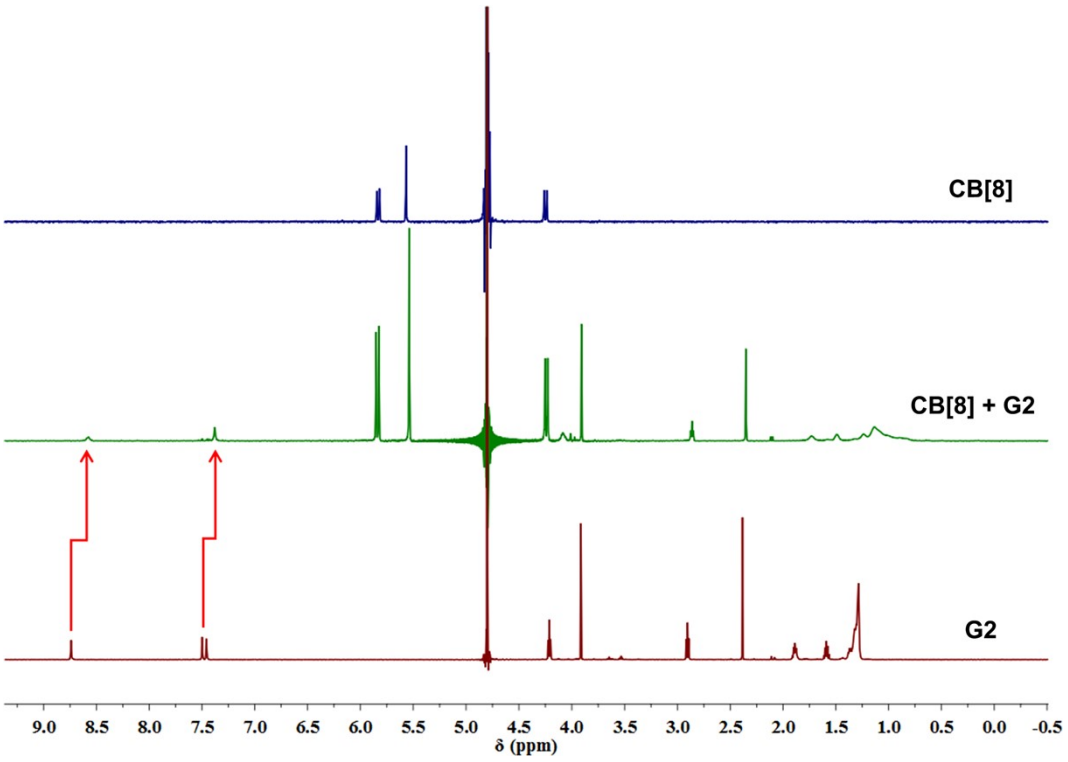

Figure S5. ^{1}H NMR spectrum (D_2O, 600 MHz, 298K) of CB[8] (saturated solution), CB[8] (1 mM) and **G2** (2 mM), **G2** (2 mM).

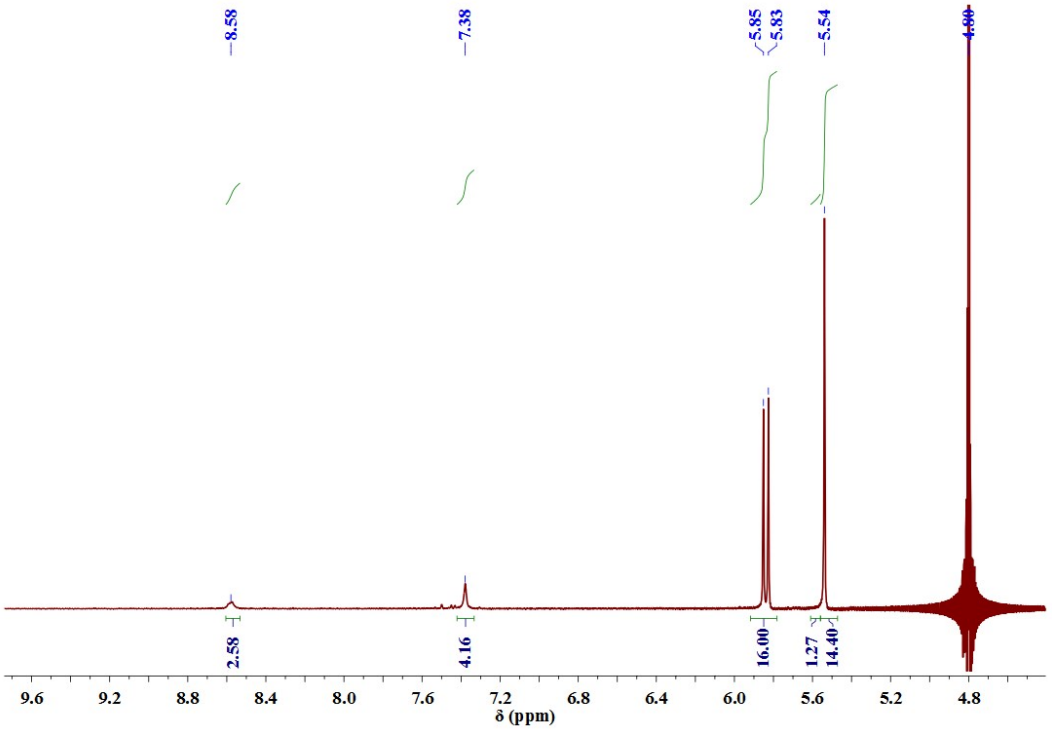

Figure S6. ^{1}H NMR spectrum (D_2O, 600 MHz, 298K) of CB[8] (1 mM) and **G2** (2 mM), confirming the 1:2 stoichiometry of CB[8] and **G2** by the integral of H.

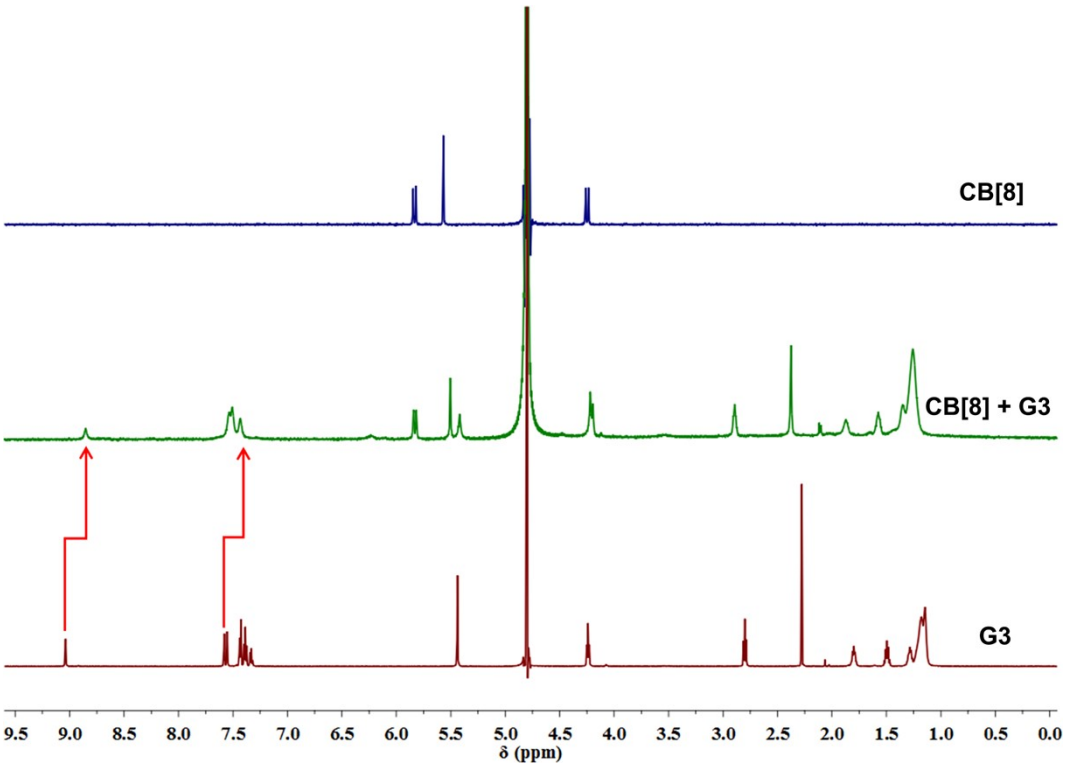

Figure S7. ^{1}H NMR spectrum (D_2O, 600 MHz, 298K) of CB[8] (saturated solution), CB[8] (1 mM) and **G3** (2 mM), **G3** (2 mM).

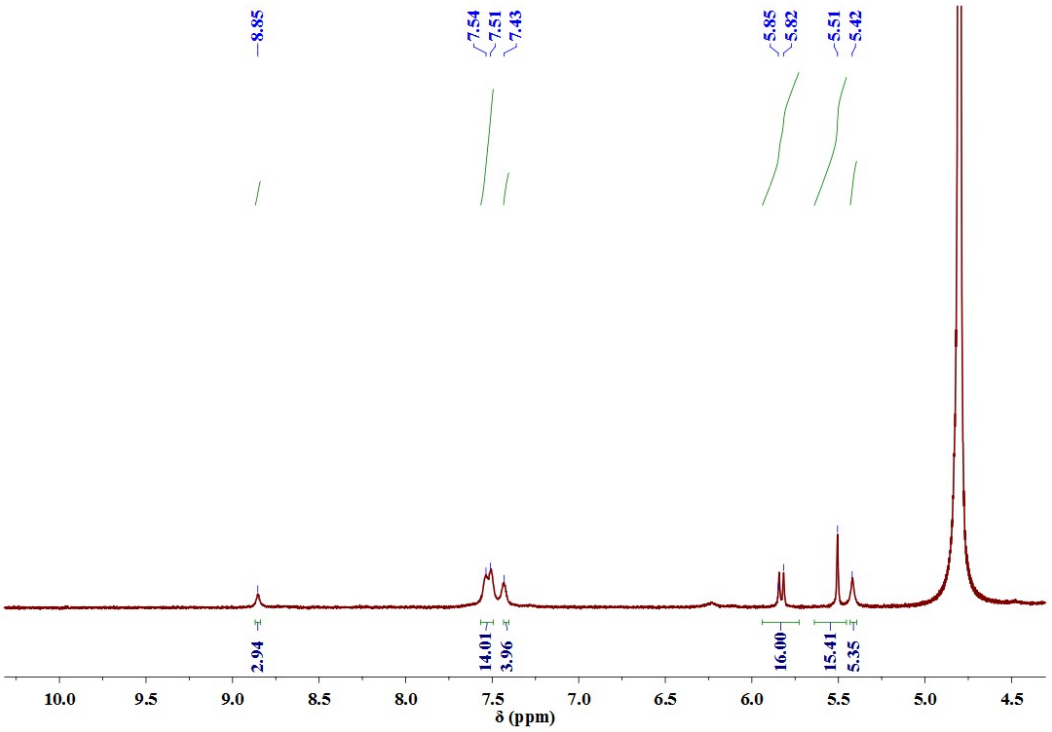

Figure S8. ^{1}H NMR spectrum (D_2O, 600 MHz, 298K) of CB[8] (1 mM) and **G3** (2 mM), confirming the 1:2 stoichiometry of CB[8] and **G3** by the integral of H.

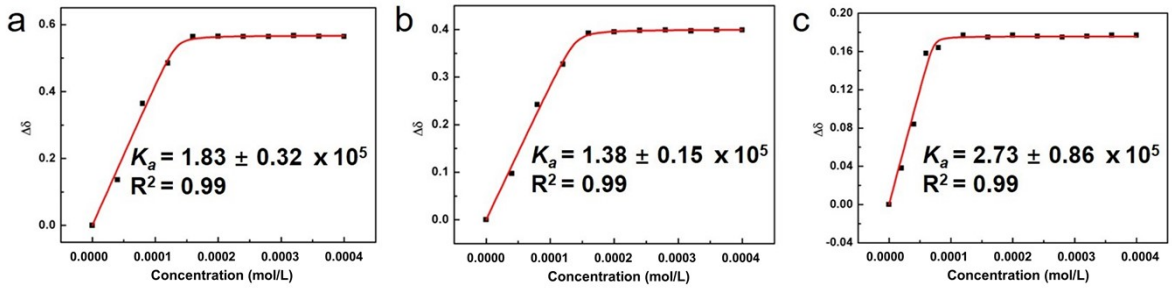

Figure S9. NMR titration curves (298 K) of (a) **G1** with CB[8] in D_2O, (b) **G2** with CB[8] in D_2O, (c) **G3** with CB[8] in D_2O. In the association constant measurement by ^{1}H NMR titration, the guest (**G1**, **G2** or **G3**) concentration was fixed at 0.1 mM. The concentration of host (CB[8]) varied from 0 to 0.2 mM. Then, ^{1}H NMR spectra were performed to record the chemical shifts. According to the nonlinear least-squares curve-fitting method, the association constant was calculated for each host-guest complex from the following equation ($\Delta\delta$ is the change of chemical shift of G at $[H]_0$, K_1 is the first stepwise association constant; K_2 is the second stepwise association constant, δ_{HG} is the NMR resonance of the complex HG; δ_{HG_2} is the NMR resonance of the complex HG_2, $\delta_{\Delta HG}$ is the change of chemical shift between δ_{HG} and δ_H, $\delta\Delta_{HG_2}$ is the change of chemical shift between δ_{HG_2} and δ_H:

$$\Delta\delta=(\delta_{\Delta HG}K_1[G]+\delta_{\Delta HG_2}K_1K_2[G]^2)/(1+K_1[G]+K_1K_2[G]^2)$$

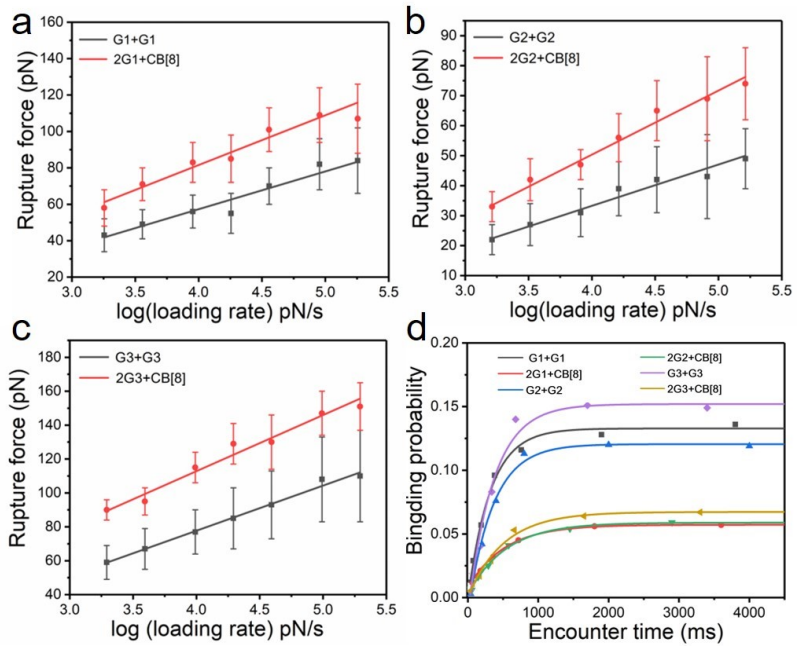

Figure S10. Dependence of the rupture forces on the loading rates. a) Rupture force between **G1** molecules with or without CB[8]. b) Rupture force between **G2** molecules with or without CB[8]. c) Rupture force between **G3** molecules with or without CB[8]. d) Binding probability plotted as a function of the encounter time.

Table S1. Summary of the binding constants between guests with or without CB[8] calculated from SMFS measurement [S6-S12].

Tested Interaction	k_{off} (s^{-1})	k_{on} ($M^{-1}\cdot s^{-1}$)	K_a (M^{-1})
G1 + **G1**	0.17	9.66	56.82
G1 + **G1** with CB[8]	0.10	22.78	227.80
G2 + **G2**	0.35	4.64	13.26
G2 + **G2** with CB[8]	0.24	14.54	60.58
G3 + **G3**	0.11	11.62	105.64
G3 + **G3** with CB[8]	0.06	36.21	603.50

According to the Evans's theory[S6-S9], k_{off} is related to the breaking force and the LR (loading rate), and calculated from the approximate form (Equation S1).

$$F_r = \frac{k_B T}{x_\beta} \ln r + \frac{k_B T}{x_\beta} \ln \frac{x_\beta}{k_B T k_{off}} \qquad \text{Equation S1}$$

where k_{off} is the kinetic off rate constant, x_β is the distance from the free-energy minimum to the barrier, and $k_B T$ is the thermal energy.

And according to the previous work of Hinterdorfer and co-workers[S10-S12],

$$k_{on} = N_A V_{eff} n^{-1} t_{0.5}^{-1} \qquad \text{Equation S2}$$

The effective concentration describes the number of binding partners (n) within the effective volume (V_{eff}) accessible for free equilibrium interaction between guest molecule attached via PEG linkers to tip and substrate: $C_{eff} = N_A^{-1} V_{eff}^{-1}$ (N_A = Avogadro's number). V_{eff} can be described as a half sphere with a free equilibrium radius (r_{eff}).

According to the Equation S1 and S2, k_{off} depends on the loading rate and the rupture force, while k_{on} is related to the concentration of guest molecules on the tip. Equation S1 and S2 are applicable for our cases.

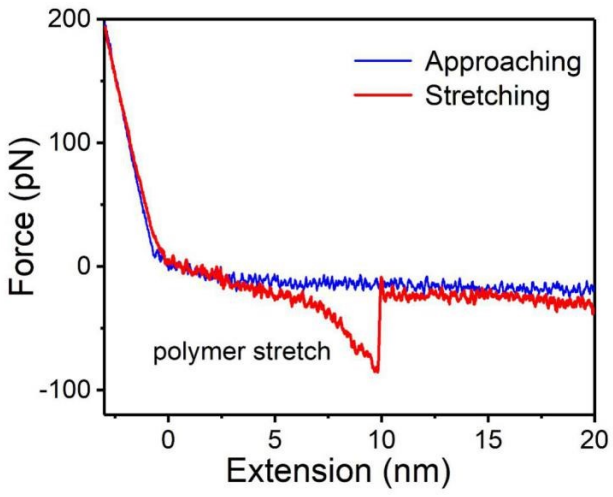

Figure S11. Typical polymer stretch curve.

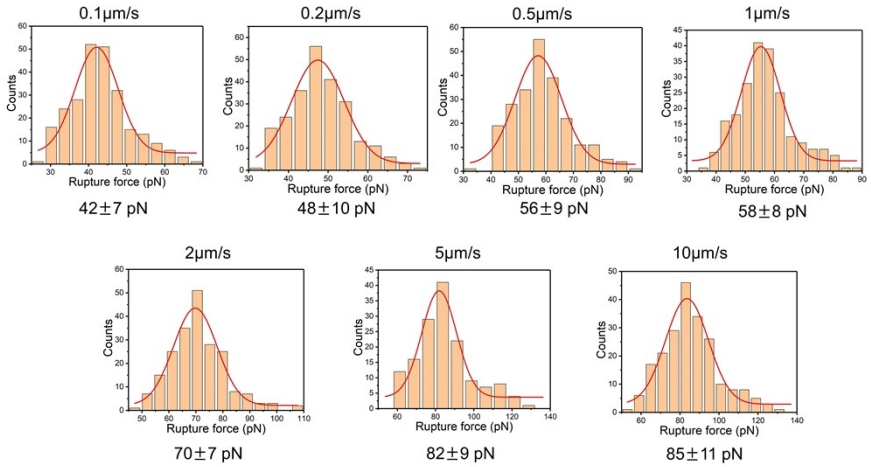

Figure S12. Rupture force between **G1** molecules depending on the loading rates.

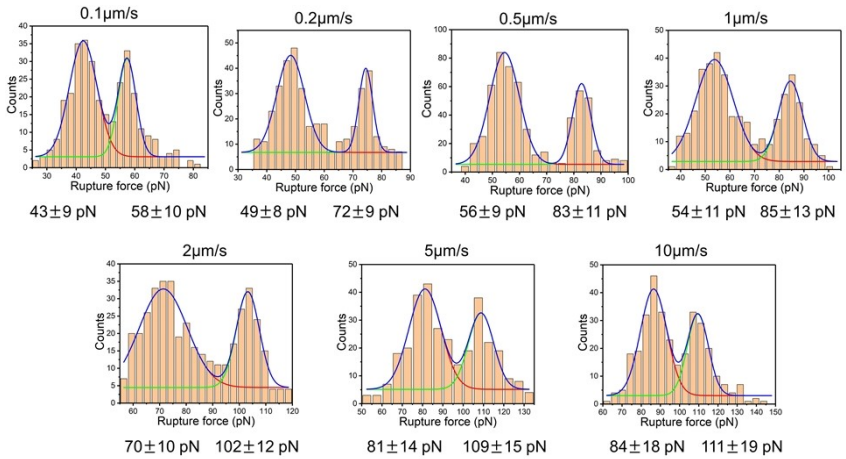

Figure S13. Rupture force between **G1** molecules with CB[8] depending on the loading rates.

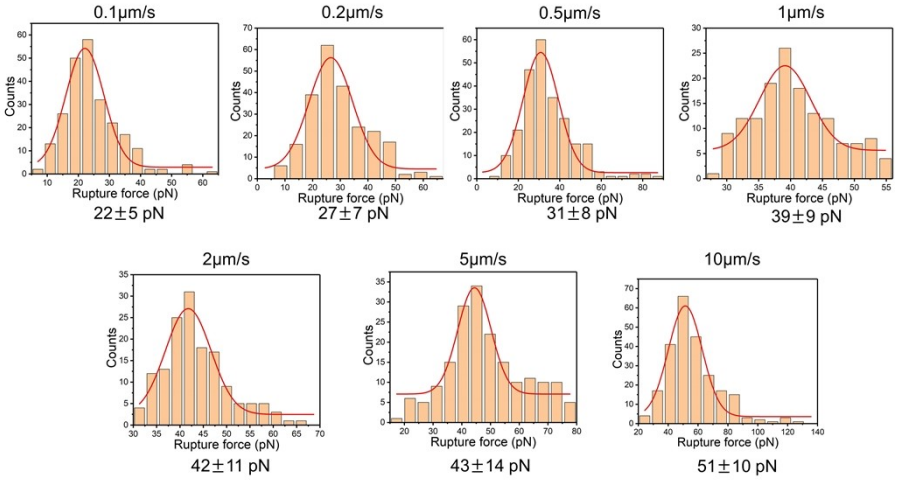

Figure S14. Rupture force between **G2** molecules depending on the loading rates.

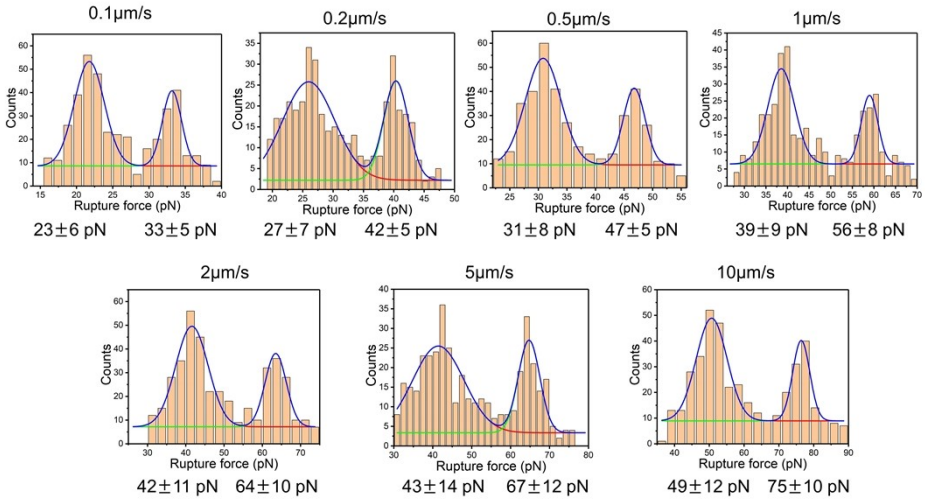

Figure S15. Rupture force between **G2** molecules with CB[8] depending on the loading rates.

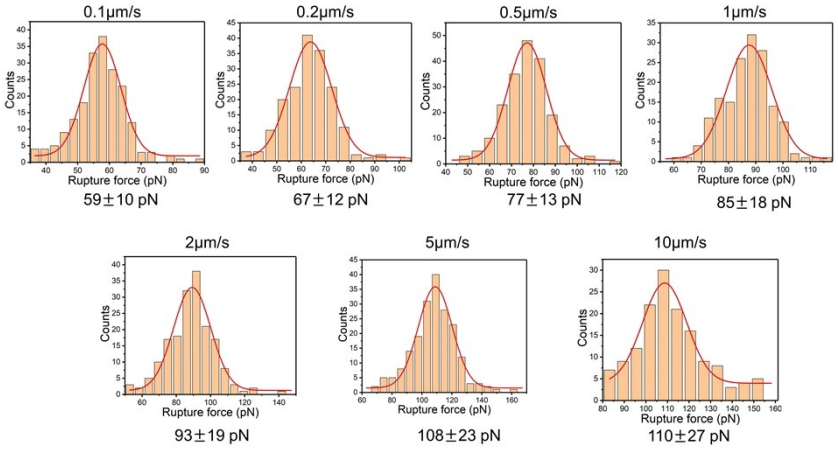

Figure S16. Rupture force between **G3** molecules depending on the loading rates.

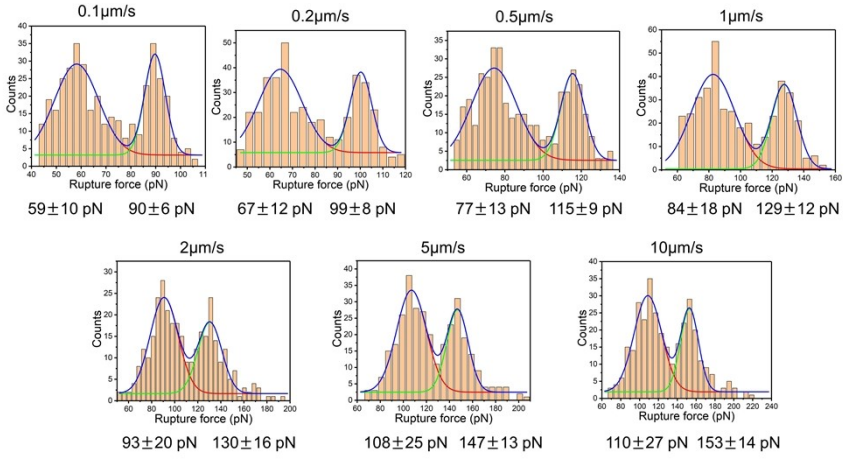

Figure S17. Rupture force between **G3** molecules with CB[8] depending on the loading rates.

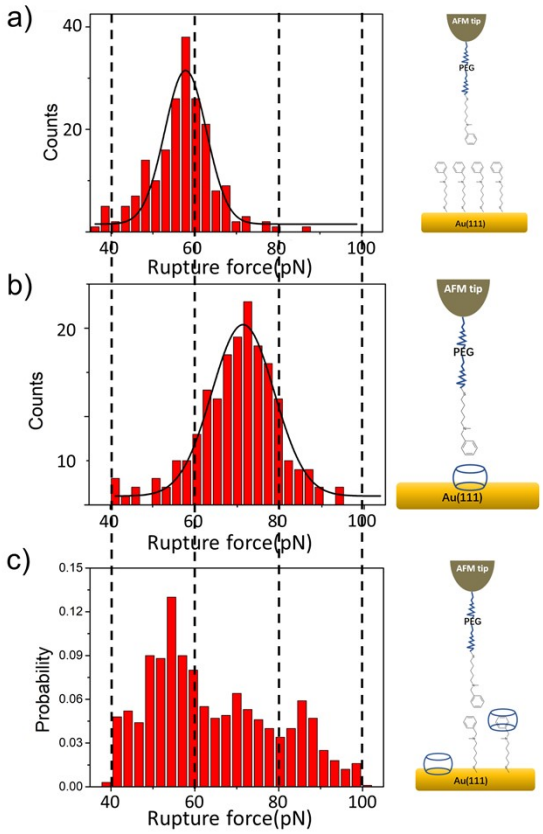

Figure S18. (a) **G1** modified substrate. The rupture force is 57±12 pN for **G1**-**G1** interaction. (b) CB[8] modified substrate. The rupture force is 72±16 pN for CB[8]-**G1** interaction. (c) CB[8] and **G1** modified substrate. Three repure forces 55±17 pN, 71±20 pN and 85±16 pN, are corresponding to **G1**-**G1**, CB[8]-**G1**, and CB[8] enhanced guest pairs interactions, respectively.

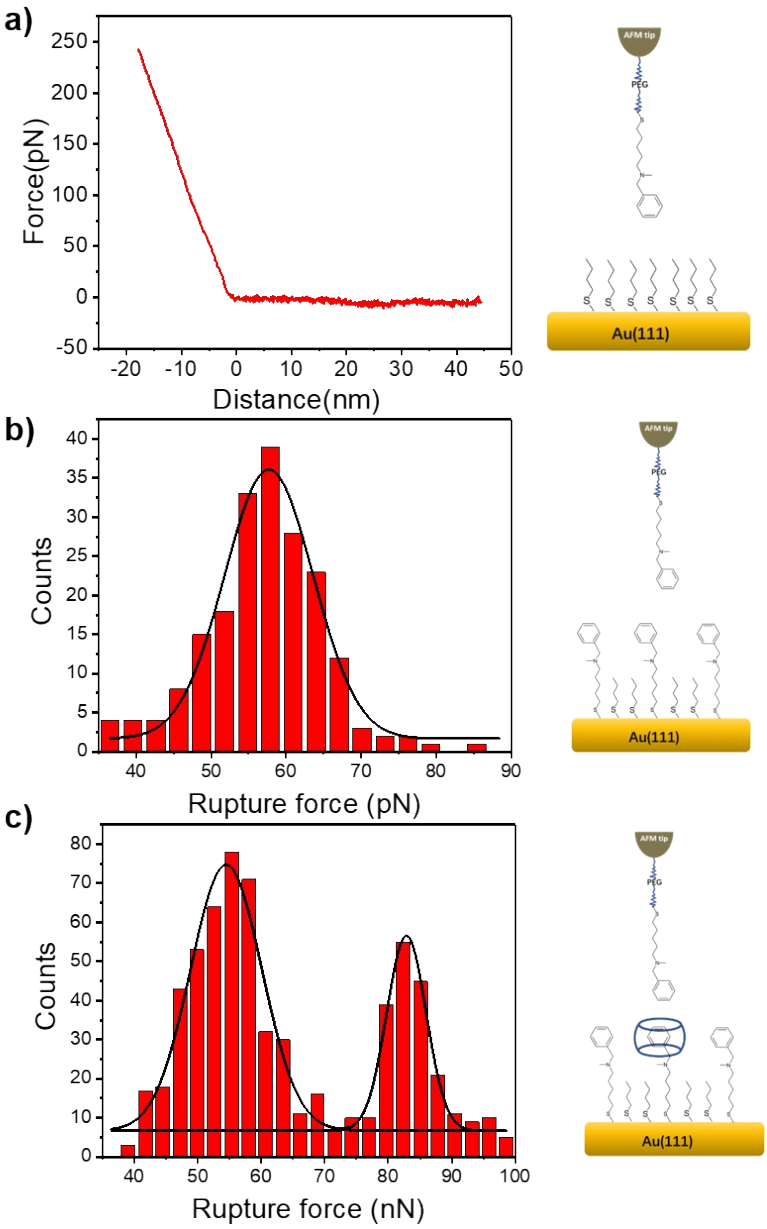

Figure S19. (a) Butanethiol modified substrate. No rupture force was determined. (b) Butanethiol and **G1** modified Au substrate and form mixed SAM. Before CB[8] addition, the rupture force is 56±9 pN for **G1**-**G1** interaction. **(c)** Butanethiol and **G1** modified Au substrate. After CB[8] addition, two rupture forces 56±12 pN and 83±11 pN, are corresponding to **G1**-**G1** and CB[8] enhanced guest pairs interactions. Mixed SAM blocked CB[8] deposition on gold substrate and diminished CB[8]-**G1** interaction.

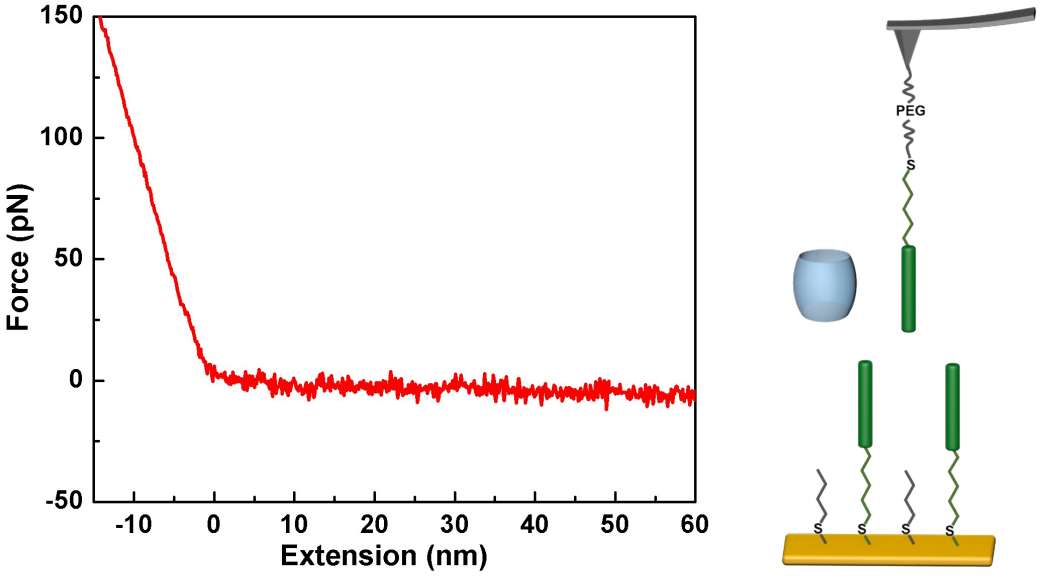

Figure S20. Stretching of **MV1** with CB[8] produced a force-extension curve showing no interaction in the test.

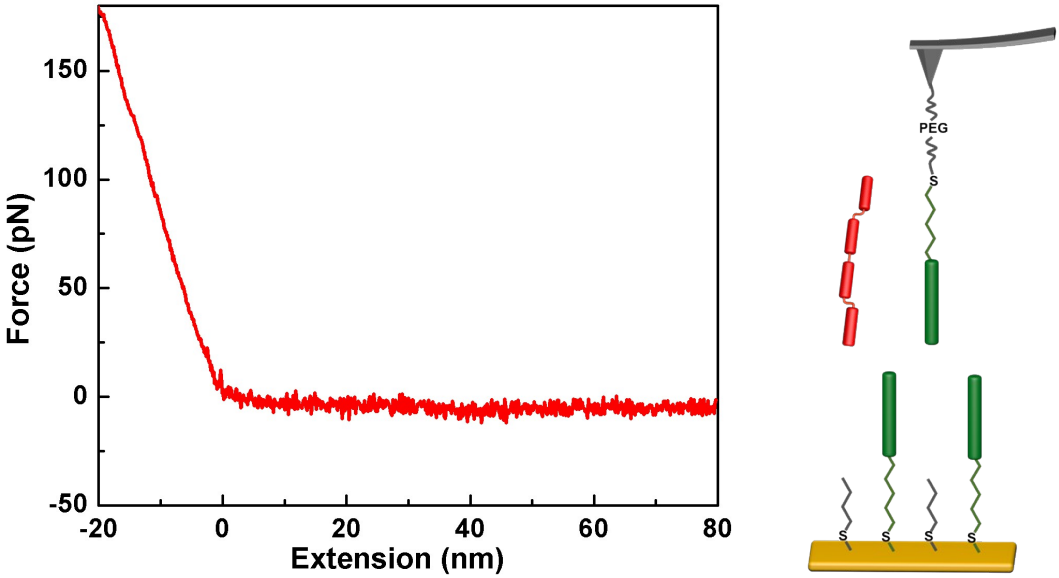

Figure S21. Stretching of **MV1** with **AZO** produced a force-extension curve showing no interaction in the test.

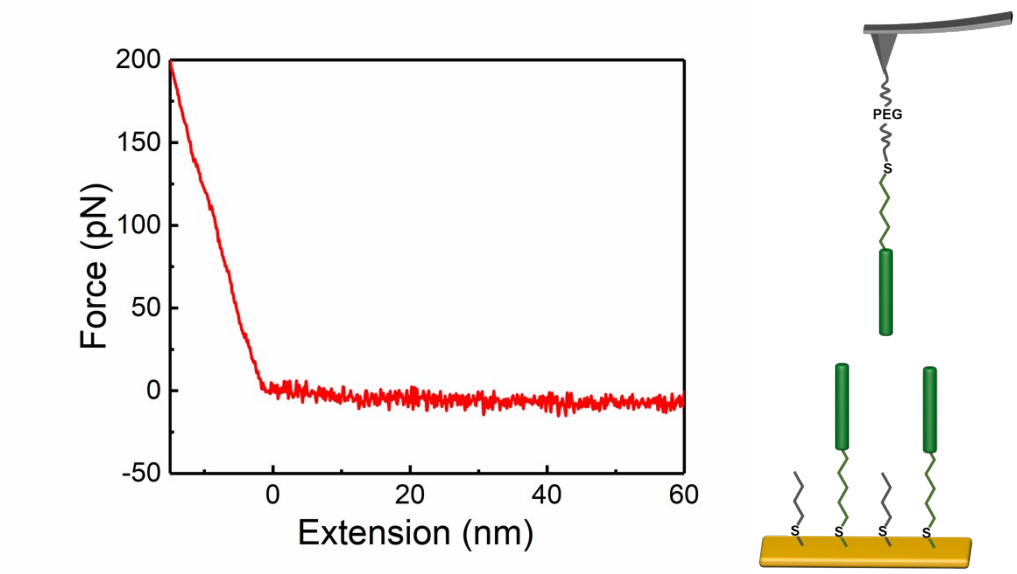

Figure S22. Stretching of **MV1** with **MV1** produced a force-extension curve showing no interaction in the test.

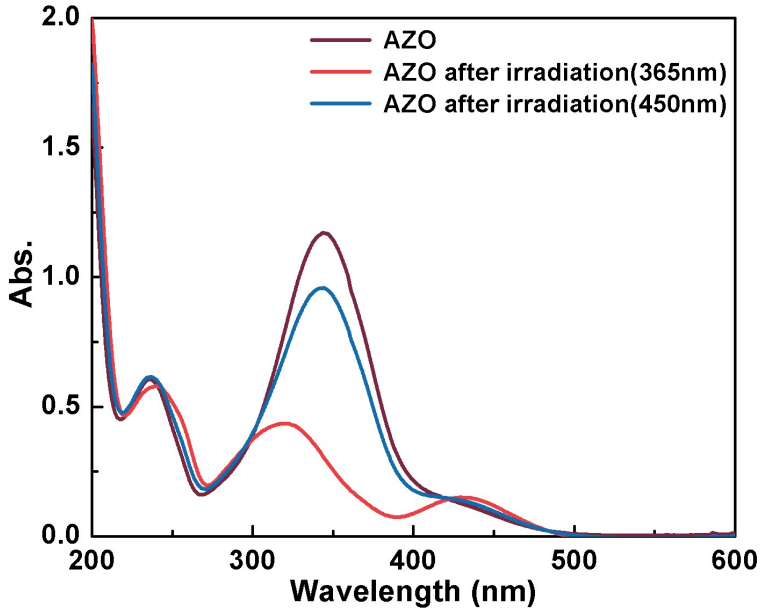

Figure S23. The UV-Vis spectra of **AZO** before and after irradiation with UV light (365 nm), and the absorbance recovered after irradiation with visible light (450 nm).

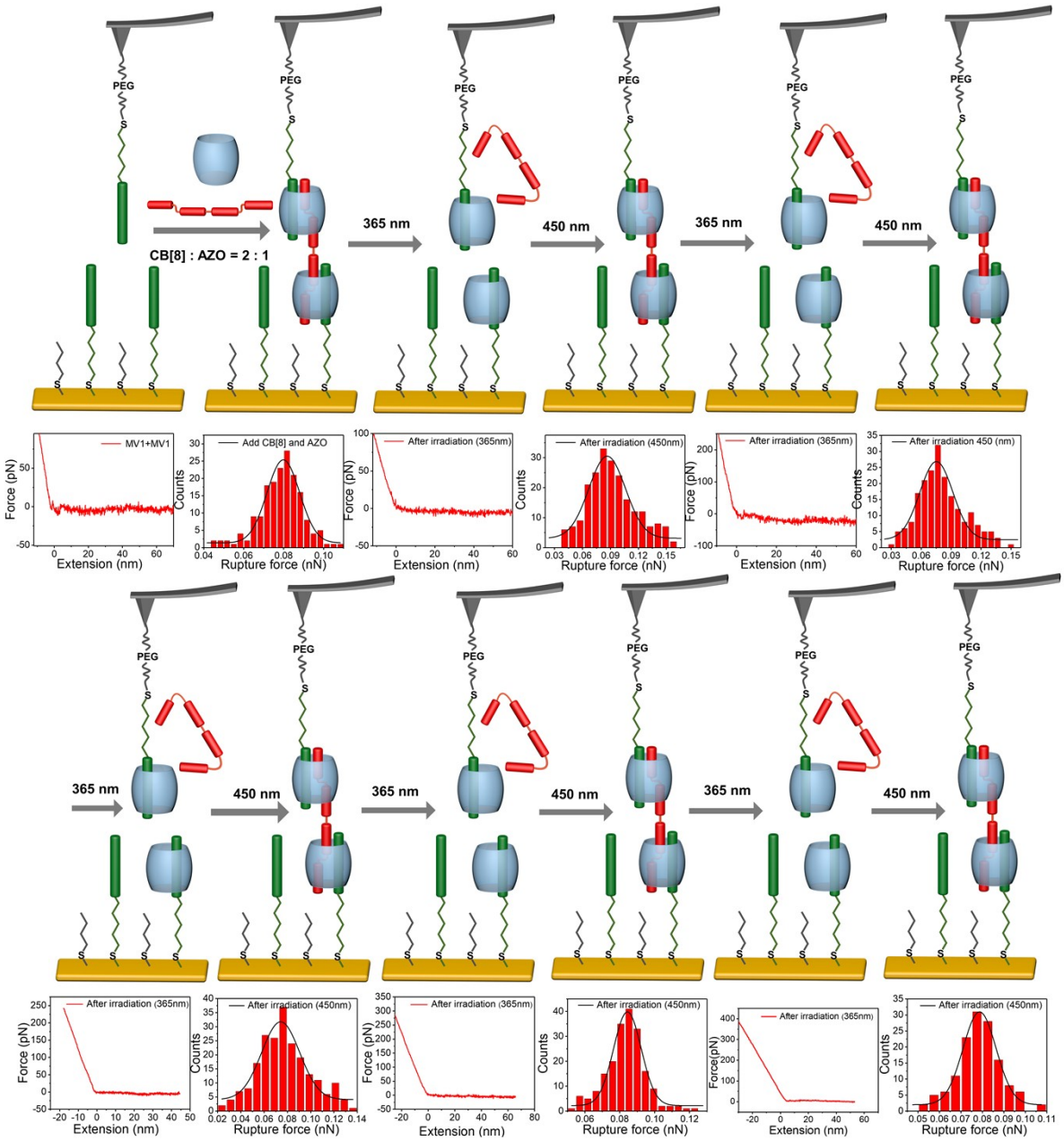

Figure S24. Schematic diagram of light reversible cycle and corresponding SMFS measurements. Typical curves showed no interaction in the test, and histograms showed the rupture force measured for the supramolecular interaction of ternary complex.

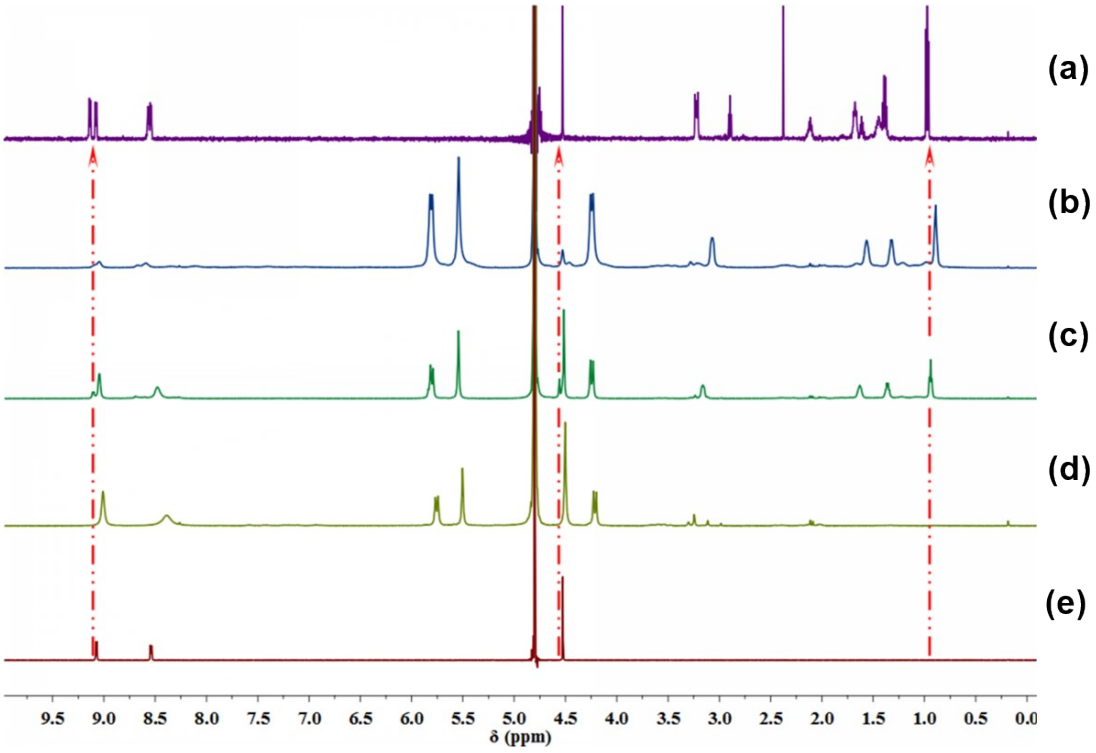

Figure S25. ^{1}H NMR spectrum (D_2O, 600 MHz, 298K) of (a) **MV1** (2 mM), (b) **MV1** (2 mM), CB[8] (2 mM) and **AZO** (1 mM), (c) MV1 (2 mM), **MV2** (2 mM), CB[8] (2 mM) and **AZO** (1 mM), (d) **MV2** (2 mM), CB[8] (2 mM) and **AZO** (1 mM), (e) **MV2** (2 mM). The weak peaks in (c) indicated that **MV1** was squeezed out of the cavity of CB[8] by **MV2**.

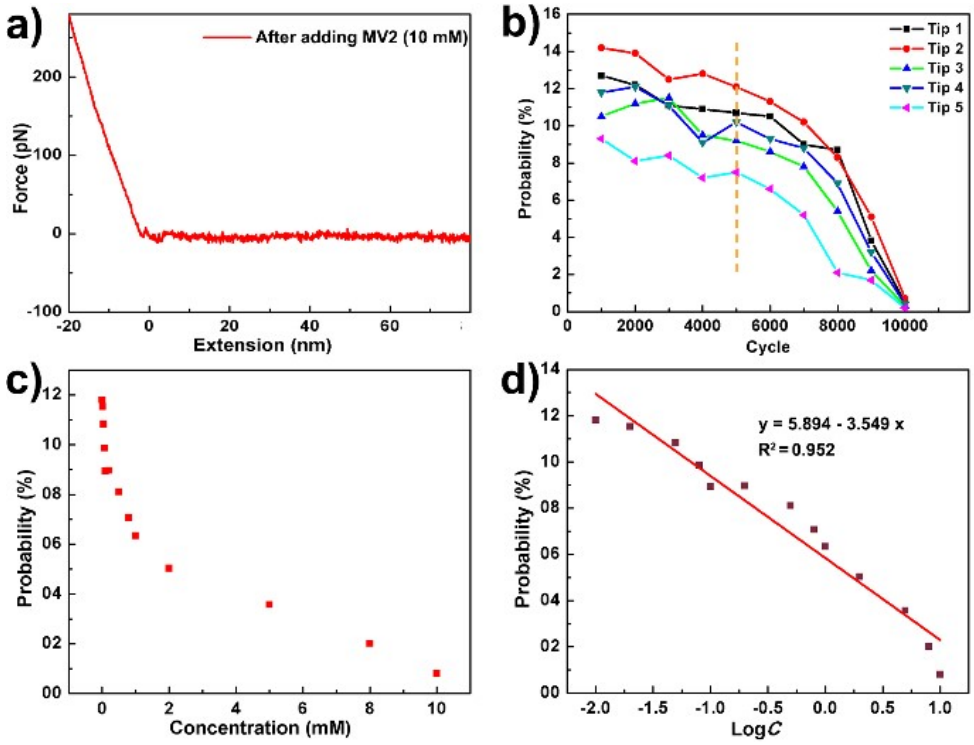

Figure S26. (a) Stretching of ternary complex of **MV1**, **AZO**, and CB[8] produced a force-extension curve showing no interaction after adding **MV2** (10 mM). (b) The probability of detectable signals during 10000 tests with the same tip. (c) Relationship between the concentration of **MV2** and the probability of detectable signals. (d) Relationship between the Log*C* (concentration of **MV2**) and the probability of detectable signals.

References

S1. H. Zhang, F. Liang and Y. W. Yang, *Chem. Eur. J.,* 2020, **26**, 198.

S2. H. Zhang, J.-R. Wu, X. Wang, X.-S. Li, M.-X. Wu, F. Liang and Y. W. Yang, *Dyes Pigm.,* 2019, **162**, 512.

S3. L. Jin, Z. Shi, X. Zhang, X. Liu, H. Li, J. Wang, F. Liang, W. Zhao and C. Zhao, *J. Mater. Chem. B,* 2019, **7**, 5520.

S4. W. Haiss, D. Lackey and J. K. Sass, *J. Chem. Phys.,* 1991, **95**, 2193.

S5. H. Clausen-Schaumann, M. Rief, C. Tolksdorf and H. E. Gaub, *Biophys. J.,* 2000, **78**, 1997.

S6. M. Zhang, Z. Gong, W. Yang, L. Jin, S. Liu, S. Chang and F. Liang, *ACS Appl. Nano Mater.,* 2020, **3**, 4283.

S7. A. Gomez-Casado, P. Jonkheijm and J. Huskens, *Langmuir,* 2011, **27**, 11508.

S8. G. I. Bell, *Science,* 1978, **200**, 618.

S9. E. Evans and K. Ritchie, *Biophys. J.,* 1997**, 72**, 1541.

S10. W. Baumgartner, H. J. Gruber, P. Hinterdorfer and D. Drenckhahn, *Single Mol.,* 2000, **1**, 119.

S11. P. Hinterdorfer, W. Baumgartner, H. J. Gruber and K. Schilcher, *PNAS,* 1996, **93**, 3477.

S12. P. Hinterdorfer, K. Schilcher, W. Baumgartner, H. J. Gruber and H. Schindler, *Nanobiology,* 1998, **4**, 177.

S13. Z. Chu, Y. Han, P. Kral and R. Klagjn, *Angew. Chem., Int. Ed.,* 2018, **130**, 7141.